Spatial entanglement in two-dimensional QCD: Renyi and Ryu-Takayanagi entropies

Yizhuang Liu[*]
Institute of Theoretical Physics, Jagiellonian University, 30-348 Kraków, Poland

Maciej A. Nowak[†]
Institute of Theoretical Physics and Mark Kac Center for Complex Systems Research, Jagiellonian University, 30-348 Kraków, Poland

Ismail Zahed[‡]
Center for Nuclear Theory, Department of Physics and Astronomy, Stony Brook University, Stony Brook, New York 11794–3800, USA

(Received 6 June 2022; accepted 10 February 2023; published 7 March 2023)

We derive a general formula for the replica partition function in the vacuum state for a large class of interacting theories with fermions, with or without gauge fields, using the equal-time formulation on the light front. The result is used to analyze the spatial entanglement of interacting Dirac fermions in two-dimensional QCD. Particular attention is paid to the issues of infrared cutoff dependence and gauge invariance. The Renyi entropy for a single interval is given by the rainbow dressed quark propagator to order $\mathcal{O}(N_c)$. The contributions to order $\mathcal{O}(1)$ are shown to follow from the off-diagonal and off mass-shell mesonic T-matrix, with no contribution to the central charge. The construction is then extended to mesonic states on the light front and shown to probe the moments of the partonic PDFs for large light-front separations. In the vacuum and for small and large intervals, the spatial entanglement entropy following from the Renyi entropy is shown to be in agreement with the Ryu-Takayanagi geometrical entropy using a soft-wall AdS_3 model of two-dimensional QCD.

DOI: 10.1103/PhysRevD.107.054010

I. INTRODUCTION

Quantum entanglement is paramount in quantum mechanics. It follows from the fact that quantum states are mostly superposition states and two acausally related measurements can be correlated. A quantitative measure of this correlation is given by the entanglement entropy, with a number of applications in quantum many-body systems and also quantum field theory [1–7].

The increase interest in entanglement, especially in lower dimensional systems, is partly motivated by recent developments in quantum information theory. Of particular interest is the concept of entanglement entropy as a measure of quantum information flow [8,9]. There is a large effort currently underway for a better theoretical and experimental understanding of entanglement in the nuclear many-body problem [10], the prompt thermalization at the RHIC [11–15], hadron tomography through DIS [15–17], and parton-parton scattering at low-x [11,16,18–22].

Recently, we have shown how entanglement in longitudinal parton-x, and also in rapidity space or $\ln\frac{1}{x}$, can be used to gain more insights on the partonic PDFs (large-x) and structure functions (small-x) using two-dimensional QCD. Recall tha 2D QCD is solvable in the large number of colors limit [23,24]. This allows for a quantitative understanding of the role played by the entanglement entropy for single meson states or their stringy form by resummation along a Regge trajectory. Remarkably, the entanglement entropy carried by a 2D nucleus on the light front (LF) shows a growth rate with rapidity at the current bound on quantum information flow.

Spatial entanglement in interacting theories, and especially gauge theories, is challenging. The geometrical construction proposed by Ryu-Takayanagi [25] in the context of a holographic dual gauge theory at large N_c and strong gauge coupling in this sense is rather remarkable. In interacting gauge theories with fermions, the dual descriptions are only approximate, and using them to analyze the

[*]yizhuang.liu@uj.edu.pl
[†]maciej.a.nowak@uj.edu.pl
[‡]ismail.zahed@stonybrook.edu

entanglement geometrically is interesting especially if large N_c arguments can be used for comparison.

Entanglement in two-dimensional QCD is intricate, as it involves interacting fermions with a dynamical gauge field. To address it, we use the replica construction in *real time*, by duplicating Minkowski space-time n times and then gluing the duplicates together using pertinent twists of the replicated fermion fields. This procedure makes the ensuing Renyi entropy, and its limiting entanglement entropy, gauge dependent in any dimension. This notwithstanding, both entropies can be evaluated by gauge fixing both in the continuum or on the lattice. For two-dimensional QCD, we will show that in the regular cutoff gauge, the large N_c results are found to be in agreement with a soft-wall holographic construction, for very small or very large intervals. For completeness, we note that a replica analysis of two-dimensional QCD was suggested in [26], using different arguments.

The paper is organized as follows: In Sec. II, we briefly review the replica construction of the Renyi entropy and its relation to the entanglement entropy. We will also recall the form of the monodromy matrix that allows for the gluing of the fermionic replicas. In particular, we will derive a new equal-time representation of the replica partition function. In Sec. III, we discuss the subtleties related to the gauge symmetry following from the gluing of the fermions, and why gauge fixing is required across the gluing cut. We will analyze the replica partition function, both in perturbation theory and in the large N_c limit of 2D QCD, in the light-front gauge. In Sec. IV, we extend our replica construction to the spatial entanglement in partonic as well as hadronic states on the light front. For the latter, the entanglement is controlled by the moments of the partonic PDFs in 2D QCD. We suggest that these moments can be extracted from the Renyi entropy for spacelike intervals in a fast moving hadron in 4D QCD using current lattice QCD simulations. In Sec. V, The leading results of the entanglement entropy both for small and large intervals are shown to be compatible with the Ryu-Takayanagi entropy, using a soft-wall gravity dual to 2D QCD. Our conclusions are given in Sec. VI.

II. REPLICA PARTITION FUNCTION AND RENYI ENTROPY

Let ρ be the density of a pure state defined in a Hilbert space composed of two complementary regions I and its complementary $\bar{I}$. For simplicity, we first focus on spatial regions. The projected or reduced density matrix in $\bar{I}$ obtained by tracing over I is [5,7]

$$\rho_I = \mathrm{Tr}_{\bar{I}}\rho. \tag{1}$$

Although ρ carries zero von Neumann entropy, ρ_I does not,

$$S = -\mathrm{Tr}_I(\rho_I \log \rho_I) \tag{2}$$

which is a measure of the quantum entanglement between I and $\bar{I}$ in ρ. To evaluate (2) one uses the Replica trick introduced in [2,3] through the Renyi entropy S_n

$$S_n = \frac{1}{1-n}\ln \mathrm{tr}\rho_I^n \equiv \frac{1}{1-n}\ln Z_n. \tag{3}$$

If Z_n is analytic in n in a neighborhood of $n=1$ with the Taylor-expanded form,

$$\ln Z_n = (n-1)Z^{(1)} + (n-1)^2 Z^{(2)} + \cdots, \tag{4}$$

then the Shannon entropy or the entanglement entropy can be simply identified as

$$S = \lim_{n\to 1} S_n = -Z^{(1)} = -\lim_{n\to 1}\frac{\partial}{\partial n}\ln Z_n. \tag{5}$$

We now show how to derive the replica partition function using the equal time formulation, valid for any interacting fermionic theory in any dimension.

A. Fermionic monodromy

Using the transfer matrix, one can show [2–4,7] that Z_n for integer value of n can be rewritten as an Euclidean path integral with fields living in a replica space, more specifically, a path integral with n identical copies of the original Euclidean space glued together along the single spatial cut corresponding to the region I with twisted fermionic boundary conditions.

For a fermionic theory one has for $i = 1, \ldots n$ replicated fermions ψ_i, each living in its own manifold; this patching corresponds to twisting the fermions in going from one patch to the other [5,7]

$$[\mathcal{T}_n]\begin{pmatrix}\psi_1\\ \psi_2\\ \vdots\\ \psi_n\end{pmatrix} = \begin{pmatrix} 0 & 1 & 0 & \cdots & 0\\ 0 & 0 & 1 & \cdots & 0\\ \vdots & \vdots & \ddots & \vdots & 1\\ (-1)^{n+1} & 0 & 0 & \cdots & 0\end{pmatrix}\begin{pmatrix}\psi_1\\ \psi_2\\ \vdots\\ \psi_n\end{pmatrix}. \tag{6}$$

The eigenvalues of the monodromy $\mathcal{T}_n$ are the n roots of unity $e^{i2\pi k/n}$ with $k = -\frac{n-1}{2}, \ldots, +\frac{n-1}{2}$. This amounts to n-multivalued fermions in a single-cut space $I = [a_1, a_2]$, with each species ψ_k picking a phase $e^{i2\pi k/n}$ in circling the left edge (a_1) of the cut clockwise, and $e^{-i2\pi k/n}$ in circling the right edge (a_2) of the cut counterclockwise.

B. Equal-time representation of Z_n

In a Hamiltonian formulation of the replica in Minkowski signature, the gluing conditions are the new

and key elements to add to the original field theory. We first consider the case of only fermionic theories with a single spatial cut, and the gluing conditions for the fermions given in (6). To construct the replica partition function for the vaccum of interacting fermions, we start from the generic off-diagonal matrix element of the vacuum density matrix $|\Omega\rangle\langle\Omega|$

$$\langle\psi_{0^-}|\Omega\rangle\langle\Omega|-\psi_{0^+}\rangle=\langle\Omega|\psi_{0^+}\rangle\langle\psi_{0^-}|\Omega\rangle, \tag{7}$$

where $|\psi_{0^\pm}\rangle$ refers to two generic fermionic coherent states (their precise relation to the single space-time cut and labeling will be detailed below). Here $|\Omega\rangle$ refers to the lowest energy state, prepared using the long time evolution, with the full fermionic Hamiltonian $H(\psi^\dagger,\psi)$

$$|\Omega\rangle=e^{-iH[\psi^\dagger,\psi]\frac{T}{2}(1-i0)}|\psi_{-\infty}\rangle, \tag{8}$$

starting from an arbitrary asymptotic coherent state $|\psi_{-\infty}\rangle$, whose explicit form is not needed. The additional minus sign in (7) is due to the Grassmannian nature of the states, when moving $\langle\psi_{0^-}|\Omega\rangle$ from left to right. Also, it is important that the density matrix $|\Omega\rangle\langle\Omega|$ is bosonic, namely, when expanded as polynomials in the Grassmannians, the order of each term must be even.

With this in mind, and to proceed to a path integral, we use the decomposition

$$e^{-iHT/2}=e^{-iH\epsilon}e^{-iH\epsilon}e^{-iH\epsilon}\ldots e^{-iH\epsilon}$$

and insert the completeness relation between any of the two evolution operators

$$\mathbf{1}=\int d\bar\psi_t d\psi_t e^{-\bar\psi_t\psi_t}|\psi_t\rangle\langle\psi_t|. \tag{9}$$

As a result, the matrix element in (7) can be cast in a standard path-integral form

$$\langle\Omega|\psi_{0^+}\rangle\langle\psi_{0^-}|\Omega\rangle=\int\prod_t d\bar\psi_t d\psi_t e^{\sum-\bar\psi_t(\psi_t-\psi_{t-1})-i\epsilon H[\bar\psi_t,\psi_{t-1}]}, \tag{10}$$

with no $-\bar\psi_{0^+}\psi_{0^-}$ term in the exponent. Equation (10) is a path-integral representation of the density matrix in real time for a single fermion species. To represent the trace, we need the completeness relation and the trace formula

$$\mathrm{Tr}A=\int d\bar\psi d\psi e^{-\bar\psi\psi}\langle-\psi|A|\psi\rangle, \tag{11}$$

in terms of which we have

$$\begin{aligned}\mathrm{Tr}\rho_I^n=&\int\prod_{k=0}^{n-2}d\bar\psi_{k,0^-}d\psi_{k,0^-}e^{-\sum_{k=0}^{n-1}\sum_x\bar\psi_{k,0^-}(x)\psi_{k,0^-}(x)},\\&\times\prod_{k=0}^{n-1}\langle\Omega|-\psi_{k-1,0^-}(x\in I),\psi_{k,0^-}(x\notin I)\rangle\\&\times\langle\psi_{k,0^-}(x\in I),\psi_{k,0^-}(x\notin I)|\Omega\rangle,\end{aligned} \tag{12}$$

where in the last equation one has made explicit the dependence on x and $\psi_{0-1,0^-}=-\psi_{n-1,0^-}$. The above can then be represented as a path integral in the replica space-time with n replica fermions species and with the gluing boundary condition across the boundary I as indicated explicitly as in the equation above.

More specifically, the nth trace can be written as a path integral with $i=0,1,..n-1$ copies of the fermion fields $\psi_{i,t}(x)$. Here i refers to the replica index, t to the time slice and x to the spatial coordination of the Grassmannian. The twisting across the cut amounts to $\psi_{i,0^+}(x\in I)=-\psi_{i-1,0^-}(x\in I)$ for $i=1,2,\ldots n-1$ and $\psi_{-1,0^+}(x\in I)=-\psi_{n-1,0^-}(x\in I)$, as illustrated in Fig. 1. Outside the cut, we have $\psi_{i,0^+}(x\notin I)=\psi_{i,0^-}(x\notin I)$. Now, using the charge conservation of the Hamiltonian, one can flip all the Grassmannians for old $i=2k-1$,

$$\begin{aligned}&\langle\Omega|-\psi_{2k-2,0^-}(x\in I),\psi_{2k-1}(x\notin I)\rangle\langle\psi_{2k-1,0^-}(x\in I),\psi_{2k-1,0^-}(x\notin I)|\Omega\rangle\\&\quad\equiv\langle\Omega|\psi_{2k-2,0^-}(x\in I),-\psi_{2k-1}(x\notin I)\rangle\langle-\psi_{2k-1,0^-}(x\in I),-\psi_{2k-1,0^-}(x\notin I)|\Omega\rangle,\end{aligned} \tag{13}$$

and redefine for odd i (including $n-1$ if n is even)

$$\psi_{2k-1,0^-}(x)\to-\psi_{2k-1,0^-}(x). \tag{14}$$

Clearly, after these transformations, one has the alternative boundary condition $\psi_{i+1,0^+}(x\in I)=\psi_{i,0^-}(x\in I)$ for $i=0,1,2,\ldots n-2$ and $\psi_{1,0^+}(x\in I)=(-1)^{n+1}\psi_{n-1,0^-}(x\in I)$, and for $x\notin I$ one needs no sign change. In terms of the independent variables $\psi_{i,0^-}(x)$, one has in the exponential for fermions along the cut or $x\in I$,

$$\begin{aligned}&\sum_i\bar\psi_{i,1}(x\in I)\psi_{i-1,0^-}(x\in I)\\&\quad-\sum_i\bar\psi_{i,0^-}(x\in I)(\psi_{i,0^-}(x\in I)-\psi_{i,-1}(x\in I))\end{aligned} \tag{15}$$

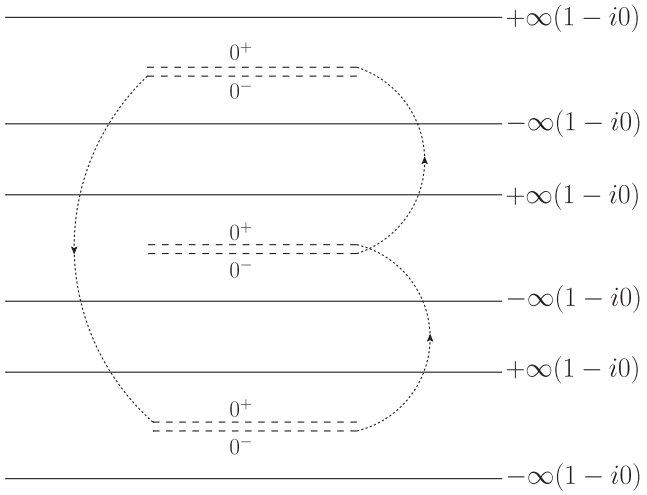

FIG. 1. Replica Minkowski space-time for $n = 3$. The boundaries for the time evolution at $t = \pm\infty(1 - i0)$ are denoted by horizontal solid lines, and the cuts at $t = 0^{\pm}$ are denoted by the double dashed lines, in the middle of each replica strip. The fields at the cut for different replica copies are glued following the dotted lines. For a thermal theory with inverse temperature β, the imaginary time version of the Euclidean space-time follows a similar construction with $\pm\infty(1 - i0) \to \pm\frac{\beta}{2}$ and periodic (or antiperiodic) boundary conditions at the solid boundaries for each replica strip.

where $\psi_{-1,0^-}(x \in I) = (-1)^{n+1}\psi_{n-1,0^-}(x \in I)$ according to the boundary condition, in addition to the Hamiltonian term

$$- i\epsilon\sum_{i,x} H\Big[\bar{\psi}_{i,1}(x), \psi_{i-1,0^-}(x \in I), \psi_{i,0^-}(x \notin I)\Big] - i\epsilon\sum_{i} H\Big[\bar{\psi}_{i,0^-}(x), \psi_{i,-1}(x)\Big]. \tag{16}$$

This finishes the derivation of the replica partition function in real time, with the twisted boundary conditions across the cut I, as illustrated in Fig. 1 for $n = 3$. Each strip in Minkowski space-time is cut at the initial times $t = 0^{\pm}$, which is shown in dashed lines, with the fermionic field assignments $\psi_{i,0^{\pm}}(x \in I)$.

To proceed further, we switch to the fermionic fields labeled by k that diagonalize the monodromy (6) for the original replica fields labeled by i

$$\psi_{k,t}(x) = \frac{1}{\sqrt{n}}\sum_{i=0}^{n-1} e^{-i\frac{2\pi k}{n}i}\psi_{i,t}(x), \tag{17}$$

$$\psi^{\dagger}_{k,t}(x) = \frac{1}{\sqrt{n}}\sum_{i=0}^{n-1} e^{i\frac{2\pi k}{n}i}\psi^{\dagger}_{i,t}(x), \tag{18}$$

at every space-time point, in terms of which the partition function reads

$$\int\prod_{k,x} d\bar{\psi}_{k,0^-}(x)d\psi_{k,0^-}(x)e^{-\sum_{k,x}\bar{\psi}_{k,0^-}(x)\psi_{k,0^-}(x)}\langle\psi_{\infty}|e^{-iH[\bar{\psi}_{k,0^-},\psi_{k,0^-}]T/2}|\psi_{k,0^-}(x \in I)e^{\frac{2\pi ik}{n}}, \psi_{k,0^-}(x \notin I)\rangle \times\langle\psi_{k,0^-}(x)|e^{-iH[\bar{\psi}_{k,0^-},\psi_{k,0^-}]T/2}|\psi_{-\infty}\rangle. \tag{19}$$

Here

$$H[\bar{\psi}_{k,0^-},\psi_{k,0^-}] = \sum_i H[\bar{\psi}_{i,0^-},\psi_{i,0^-}] \tag{20}$$

refers to the Hamiltonian for n identical copies of the original Hamiltonian, written in the new variables ψ_k, which is seen to satisfy the identity

$$|\psi_{k,0^-}(x, \in I)e^{\frac{2\pi ik}{n}}, \psi_{k,0^-}(x \notin I)\rangle = e^{i\frac{2\pi k}{n}\sum_k\sum_{x\in I}\psi^{\dagger}_{k,0^-}(x)\psi_{k,0^-}(x)}|\psi_{k,0^-}(x)\rangle. \tag{21}$$

Equation (19) reduces to the expectation value

$$\langle\Omega_n|\exp\left[i\sum_k\frac{2\pi k}{n}\int_{x\in I}dx\psi^{\dagger}_{k,0^-}(x)\psi_{k,0^-}(x)\right]|\Omega_n\rangle, \tag{22}$$

I refers to the cut, and $|\Omega_n\rangle$ is simply a tensor product of n identical vacua of the original theory, one for each replica copy labeled by i. Note that the exponential is the equal-time charge density in k-space, conjugate to the replica i space

$$\int_{x\in I}dx\psi^{\dagger}_{k,0^-}(x)\psi_{k,0^-}(x) \equiv \int_{x\in I}dxj_{0,k}(x). \tag{23}$$

From here on, the argument x is short for the equal-time argument $(0^-, x)$ unless specified otherwise. In terms of the original replica fields labeled by i, (22) reads

$$Z_n = \langle\Omega_n|\exp\left[i\sum_{i,j}\sum_k\frac{2\pi k}{n^2}e^{i\frac{2\pi k}{n}(i-j)} \times\int_{x\in I}dx\psi^{\dagger}_i(x)\psi_j(x)\right]|\Omega_n\rangle. \tag{24}$$

Equation (24) is the replica partition function or the n trace of the reduced density matrix. It is an expectation value of equal-time operators in a replica theory with n copies.

For a free fermion theory, (22) reduces to the result established in [5], based on the interpretation of the replica boundary conditions as background magnetic fields with fluxes $\frac{2\pi k}{n}$. Indeed, analytically continuing (22) to Euclidean signature and using the 2D bosonization relation $\psi_k^\dagger \gamma^\mu \psi_k = \frac{1}{\sqrt{\pi}} \epsilon^{\mu\nu} \partial_\nu \phi_k$, we have

$$\begin{aligned} & i \sum_k \frac{2\pi k}{n} \int_{x\in I} dx \psi^\dagger_{k,0^-}(x) \psi_{k,0^-}(x) \\ & \equiv i \sum_k \frac{\sqrt{4\pi} k}{n} \left[\phi_k(a_2) - \phi_k(a_1) \right] \\ & \equiv -i \sum_k \int d^2x A^k_\mu(x) \bar{\psi}_k(x) \gamma^\mu \psi_k(x), \end{aligned} \tag{25}$$

with the replica magnetic fields

$$\epsilon_{\mu\nu} \partial^\mu A^{k,\nu}(x) = \frac{2\pi k}{n} [\delta^2(x - a_1) - \delta^2(x - a_2)],$$

in agreement with [5]. However, our result (24) is more general, as it applies to generic interacting fermionic systems in Minkowski signature, including 4-Fermi or gauge interactions.

In sum, we derived an equal time representation for the replica partition function $Z_n = e^{(n-1)S_n}$ for any free or interacting two-dimensional fermionic theory, along an equal-time spacelike cut. It readily generalizes to any dimensions $D + 1$ for any D-dimensional spacelike region I. For free fermions, the above can also be derived using bosonization [27], but here we have shown that the same applies to any fermionic theory, with or without interactions. Equations (22)–(24) are the main results of this section.

III. TWO-DIMENSIONAL QCD

Now we proceed to show how the preceding result can be exploited in two-dimensional QCD, paying particular attention to issues of gauge invariance. We present a perturbative analysis of the entanglement entropy for small spatial cuts, followed by a large N_c analysis whatever the size of the cut.

A. Gauge symmetry

Each of the replicated n copies of two-dimensional QCD has local gauge invariance in the corresponding space-time and requires gauge fixing across each of the replicated cuts. More specifically, additional gauge links connecting i to $i + 1$ copies in space-time need to be specified. Indeed, the exponent in (24)

$$\int_{x\in I} dx \psi_i^\dagger(x) \psi_j(x)$$

while local in x space is off-diagonal in replica i space. While gluing the replicated space-times, the gauge transformation from one edge in the i patch, say at time 0^-, has to be adjusted so to match the gauge transformation from the other edge in the $i + 1$ patch at time 0^+. This means fixing the gauge along the cut. In two dimensions we may choose a gauge, e.g. the axial gauge or temporal gauge, where the only physical degrees of freedom are fermions, and then apply the above construction solely to the fermions. The two approaches are not necessarily equivalent. The former in terms of the gauge fields is explicitly gauge dependent, while the latter in terms of solely the fermionic fields is implicitly gauge dependent through the inverted gauge propagator. The elimination procedure of the gauge fields, does not work in higher dimensions. Finally, because of local gauge symmetry, replica partition functions lack, in general, an interpretation as the trace over a reduced density matrix in a Hilbert space viewed as a tensor product.

This notwithstanding, we may use (24) in either Minkowski or Euclidean signature as a definition of Z_n, and proceed to evaluate it either perturbatively or nonperturbatively using the planar approximation (alternatively a lattice evaluation). In all cases, gauge fixing is required. Below, we show that while Z_n and the ensuing Renyi entropy S_n are in general gauge dependent, the leading contributions at small and large cuts are gauge independent. The same results will be shown to follow from a gauge invariant holographic construction.

B. Perturbative analysis: Spatial vs LF

The representation of the fermion replica partition function as an equal-time correlation function allows generalization to any cut along the direction n^μ in a manifestly invariant manner

$$\begin{aligned} & Z_n(x^\mu = L n^\mu) \\ & = \langle \Omega_n | \mathcal{T} \exp \left[\sum_k i \frac{2\pi k}{n} \int_0^L ds n^\mu \epsilon_{\mu\nu} j^\nu_k(s n^\mu) \right] | \Omega_n \rangle, \end{aligned} \tag{26}$$

where $\epsilon_{\mu\nu} j^\nu_k(x)$ is the vector current operator for the fermion ψ_k. This representation is manifestly Lorentz invariant. Therefore, the partition function $Z_n(x)$ depends only on the Lorentz invariant length $\sqrt{-x^2}$ of the separation, not the direction. Furthermore, assuming that $j^\nu_k(x)$ satisfies the standard local commutation relations, one can show that the $Z_n(x)$ should have the same analyticity properties, in particular the domain of analyticity, and the $i\epsilon$ prescription as a two-point function of local scalar fields.

1. Spacelike interval

The representation as a correlation function allows a perturbative expansion using standard Feynman rules. For a free fermion, this reproduces the well-known result for the

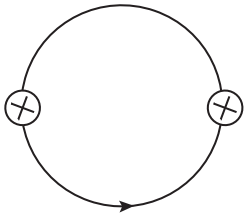

FIG. 2. The vacuum polarization contribution to $\ln Z_n$ in Eq. (19). The crossed dots denote insertions of the operator $\int dx\psi^\dagger\psi$. For massless free fermions, it is the only nonvanishing diagram and contributes to the known $c=\frac{N_c}{3}$. For a superrenormalizable theory, this is the only diagram that contains a UV divergence.

entanglement entropy of a spacelike interval $[0,L]$. Indeed, if one considers $\ln Z_n$, then only the connected diagrams will contribute

$$\ln Z_n(L) = \sum \text{connected diagrams with insertions of } \int dx\psi^\dagger\psi. \tag{27}$$

For a free fermion, this means loops with arbitrary numbers of $\bar\psi_k\gamma^0\psi_k$ insertions. However, due to the absence of anomalies for any fermion loop with more than three fermion propagators, an application of the vector and axial Ward identities shows that all loops (with more than three insertions) vanish. The only nonvanishing diagram is the vacuum polarization diagram shown in Fig. 2 at the origin of the 2D axial anomaly. A direct calculation leads to the standard central charge $\frac{N_c}{3}$.

More specifically, the vacuum polarization diagram in Fig. 2 contributes as

$$\ln Z_n|_{\text{bubble}} = \frac{N_c}{2}\sum_k\left(\frac{2\pi k}{n}\right)^2\int\frac{d^2p}{(2\pi)^2}\Pi^{00}(p) \times\frac{2-2\cos p^z L}{(p^z)^2}. \tag{28}$$

For a massive fermion one has the well-known vacuum polarization in $2D$

$$\Pi^{00}(p)=\frac{(p^z)^2}{\pi}\int_0^1 dx\frac{1}{p^2+\frac{m^2}{x(1-x)}}, \tag{29}$$

with the result

$$\ln Z_n|_{\text{bubble}} = -\frac{(n^2-1)N_c}{12n}\int_0^1 dx\int_{-\infty}^{\infty}dp^z\frac{1-\cos p^z L}{\sqrt{p_z^2+\frac{m^2}{x(1-x)}}}. \tag{30}$$

The first term diverges in the UV. Using the UV regulator

$$1-\cos p_z L\to\cos p_z a-\cos p_z L,$$

the result is

$$\ln Z_n|_{\text{bubble}} = -\frac{(n^2-1)N_c}{6n}\int_0^1 dx\left[K_0\left(\frac{ma}{\sqrt{x(1-x)}}\right) - K_0\left(\frac{mL}{\sqrt{x(1-x)}}\right)\right], \tag{31}$$

with the Renyi entropy (3) in the form

$$S_n=\frac{(n+1)N_c}{6n}\int_0^1 dx\left[K_0\left(\frac{ma}{\sqrt{x(1-x)}}\right) - K_0\left(\frac{mL}{\sqrt{x(1-x)}}\right)\right]\to\frac{N_c}{3}\ln\left(\frac{L}{a}\right). \tag{32}$$

The rightmost result follows in the massless limit ($m\to 0$) for $n=1$. The L-dependent central charge is

$$c_n(L)=L\frac{dS_n}{dL}=\frac{(n+1)N_c}{6n}\int_0^1 dx\frac{mLK_1\left(\frac{mL}{\sqrt{x(1-x)}}\right)}{\sqrt{x(1-x)}}, \tag{33}$$

which is seen to decay exponentially as $N_c e^{-2mL}$ at large L. The Renyi entropy (32) at large L is dominated by the constant UV contribution

$$\frac{(n+1)N_c}{6n}\left(\int_0^1 dxK_0\left(\frac{ma}{\sqrt{x(1-x)}}\right)+\mathcal{O}(e^{-2mL})\right) \to\frac{(n+1)N_c}{6n}\left(\ln\left(\frac{C}{ma}\right)+\mathcal{O}(e^{-2mL})\right). \tag{34}$$

Since the interaction is superrenormalizable (valid also for 2D QED), any diagram with interactions vertices will be less singular than the vacuum polarization diagram. In other words, they are UV free and contribute $\mathcal{O}(g^{2n}L^{2n})$ at short distances. The dominant contribution at small L is therefore

$$S(L)=\frac{N_c}{3}\ln\frac{L}{a}+\mathcal{O}(g^2L^2). \tag{35}$$

On the other hand, we expect exponential decay with L at large L, for massive fermions.

Finally, we note that for two disjoint intervals, the above formalism allows the calculation of the so-called mutual information,

$$\ln Z_n(L_1 \cup L_2) - \ln Z_n(L_1) - \ln Z_n(L_2) = \sum \text{connected diagrams with both insertions in } L_1 \text{ and } L_2. \tag{36}$$

Since the distance between L_1 and L_2 is nonzero, the diagrams have a natural UV cutoff and will be convergent. Moreover, at large separation d between L_1 and L_2, the mutual information decays exponentially as e^{-2md} in massive theories. This applies even to superrenormalizable theories (Gross-Neveu) after coupling constant renormalization. However, for 2D QCD in axial gauge, the mutual information is clearly gauge dependent as well, and suffers from the same shortcomings observed for the entanglement entropy as well.

2. Lightlike interval

For lightlike intervals, the analysis proceeds similarly. For that, consider the light-front spatial direction x^- with a fixed interval $[0, L^-]$. In the light-cone gauge, the LF time evolution can be represented as a path integral, for which we need to evaluate

$$\left\langle \exp\left[\sum_{ij}\sum_{k} i\frac{2\pi k}{n} e^{i\frac{2\pi k}{n}(i-j)} \times \int_0^{L^-} dx^- \psi_i^\dagger(0,x^-)\psi_j(0,x^-)\right]\right\rangle_{\text{int}}. \tag{37}$$

But since the equal LF time field is equivalent to a free field, the above is the same as the noninteracting theory. All the vacuum diagrams with a typical contribution shown in Fig. 3, vanish due to the fact that $H_{\text{int}}|0\rangle_{\text{free}} = 0$.

For a free fermion on the LF, a rerun of the preceding arguments yields

$$\ln Z_n|_{\text{bubble}} = \frac{N_c}{2}\sum_k \left(\frac{2\pi k}{n}\right)^2 \int \frac{d^2p}{(2\pi)^2}\Pi^{++}(p) \times \frac{2-2\cos p^+L^-}{(p^+)^2}, \tag{38}$$

with the polarization function for the *good* fermion

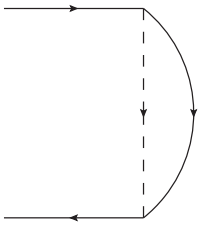

FIG. 3. A typical vacuum insertion in 2D QCD that vanishes in LF perturbation theory.

$$\Pi^{++}(p) = \frac{(p^+)^2}{\pi}\int_0^1 dx \frac{1}{p^2 + \frac{m^2}{x(1-x)}}. \tag{39}$$

The integral in p^- can be carried explicitly, with the result

$$\ln Z_n = -\frac{(n^2-1)N_c}{12n}\int_0^1 dx \int_0^\infty dp^+ \frac{1-\cos p^+L^-}{p^+}. \tag{40}$$

After introducing the UV cutoff a^- as before, we have

$$S_n(L^-) \to \frac{(n+1)N_c}{12n}\ln\frac{L^-}{a^-} \to \frac{N_c}{6}\ln\frac{L^-}{a^-}, \tag{41}$$

with the rightmost result following from the $n \to 1$ limit. Note that the coefficient in (41) is half the coefficient in (32). This is due to the fact that for the spacelike interval, the left- and right-handed fermions contribute equally. On the LF, only the good component or the left-handed fermion, contributes to the entanglement entropy. This is manifest in the integration support of the integrals in (30) and (40).

The central charge for spacelike or lightlike intervals can also be calculated directly using methods in many-body physics [28]. In this case, the spatial entanglement of a free fermion can be tied to the Fermi sea. More specifically and in the rest frame, the standard half-filling Fermi sea state (the ground state for the XX model), with all the modes $-\frac{\pi}{2a} < k < \frac{\pi}{2a}$ filled, has a central charge $c = \frac{1}{3}$. In contrast and on the LF, the ground state follows by filling the negative frequencies $-\frac{\pi}{a} < k < 0$ only. The central charge is $c = \frac{1}{6}$. Indeed, following the arguments presented in [28], the function $m(k)$ related to the characteristic function $\chi(k)$ of the occupied state reads

$$m(k) = 2\chi(k) - 1 = e^{-i\pi}e^{i\text{Arg}(k)}, \tag{42}$$

with a discontinuity number $n = 1$, hence a central charge $c = \frac{n}{6} = \frac{1}{6}$. In the rest frame, the Fermi sea is symmetric around $k = 0$ with both left- and right-moving fermionic excitations at the edges. In the light front, this symmetry is broken with only right-moving fermionic excitations at the edge.

C. Summing planar contributions with replicas: Counting $n-1$

In the large N_c limit, the leading contribution is again dominated by a single planar fermion loop with possible insertions of the charge operators. We are only interested in

the leading $n-1$ contributions that lead to the entanglement entropy. Here we present a power-counting argument that eliminates most of the diagrams.

Notice that the insertions of the $\int dx\psi^\dagger\psi$ operators in each of the fermion propagators have the generic structure

$$\mathcal{G}_{i,j}(p,p') = \delta_{ij}G_0(p,p') + \sum_{m=1}^{\infty} G_m(p,p')A_{ij}^m, \tag{43}$$

where p and p' denotes the incoming and outgoing momenta, and

$$A_{ij}^n = \sum_{k=-\frac{n-1}{2}}^{\frac{n-1}{2}} e^{-i\frac{2\pi k}{n}(i-j)}\left(\frac{k}{n}\right)^n \tag{44}$$

is an ij matrix in replica space, with eigenvalues $(\frac{k}{n})^n$. For any diagram, the n dependence follows from the trace over matrices formed by A, depending on the locations and numbers of the insertions.

Now consider the generic replica-color structure shown in Fig. 4. Inside a single fermion loop there is a ladder formed by N instantaneous gluons. Let us now make insertions on the fermion propagators. The number of powers of A on each rung is labeled by (n_i, m_i) where $i = 0, 1, 2..N$. Let us show that there exits only a single i in which one of the (n_i, m_i) can be nonvanishing. Indeed, one can go from the left side by summing over i_1 and obtain

$$A_{ii}^{n_1+m_1} \propto \sum_{k=-\frac{n-1}{2}}^{\frac{n-1}{2}} \frac{k^{n_1+m_1}}{n^{n_1+m_1}}, \tag{45}$$

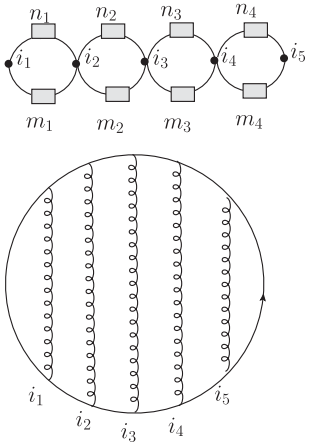

FIG. 4. A generic replica-color structure of a planar diagram that contributes to $\mathcal{O}(N_c)$. The upper diagram follows by inserting the replica fluxes (n_i, m_i) in the lower diagram, in each of the lines between the gluonic exchanges. The dotted 4-Fermi interactions labeled by the replica index i in the upper diagram is short for the integrated gluon exchange from the lower diagram in 2D.

which is independent of i, and is always proportional to $(n-1)$ as long as $n_1 + m_1 \neq 0$. Therefore, if $n_1 + m_1 \neq 0$, no other insertions are allowed. Otherwise one obtains $\delta_{i_1 i_2}$ and goes to (n_2, m_2). Continuing in this way the assertion is confirmed.

Given the rules above, it is not hard to find the diagrams that are leading in $n-1$. Indeed, a generic planar diagram can be obtained from Fig. 4 by inserting rainbowlike 1PI diagrams, on each of the fermion propagators. If the operator insertions are outside such rainbows, then the replica-color structure remains the same, and the above argument applies. Specifically, for the i ring with the insertion numbers (n_i, m_i) possibly nonzero, one may add rainbows between the insertions, without changing the counting in $n-1$. Moreover, if the insertions are inside such rainbows, then by moving the legs of the gluons along the contour, one can view the gluons inside the rainbow, as forming a ladder. The other gluons that used to be a ladder become rainbows. In this way we are again reduced to the previous case.

D. Order $\mathcal{O}(N_c)$ contribution

The diagrams that are leading have the topological structure shown in Fig. 5. In the upper diagram, at least one of T and T' is nontrivial. If one of T and T' is trivial, then the first diagram reduces to the lower one. However, notice that in these cases the T and T' themselves can be viewed as forming rainbows; therefore, the above diagrams are really equivalent to the following: arbitrary number of operators inserted in a fermion loop with arbitrary number equal or grater than 1 of rainbows inserted along the fermion propagators between them. When combined with the diagram without any rainbow insertions, the fermion propagator between the operator insertions resums to the dressed one.

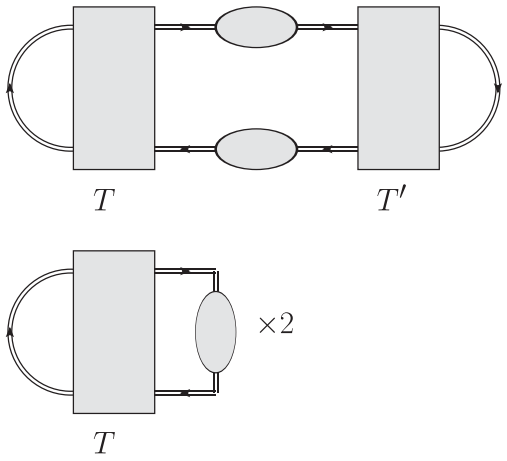

FIG. 5. The single-loop contribution. The shaded boxes are the planar two-to-two amplitudes and the insertions are located at the shaded circles. Notice that between two insertions there can be arbitrary number of rainbows.

With this in mind, the leading N_c contribution to the entanglement entropy is actually equivalent to that of a free fermion, but with a rainbow dressed propagator

$$S_{N_c} = N_c S(\langle \psi(x-y)\bar{\psi}(0)\rangle_{\text{Rainbow}}). \tag{46}$$

Here $S(G_{\text{Rainbow}}(x-y))$ denotes the entanglement entropy for a free fermion, with a rainbow dressed propagator [29,30]

$$G_{\text{Rainbow}}((x-y)) = \int \frac{d^2p}{(2\pi)^2} e^{-ip(x-y)} \frac{p^+\gamma^+ + (p^- + \frac{g^2N_c}{2\pi p^+} - Ag^2N_c\text{sign}(p^+))\gamma^- + m}{p^2 - m^2 + \frac{1}{\pi}g^2N_c - Ag^2N_c|p^+|} \tag{47}$$

with A a gauge parameter.

The fact that (46) through (47) depends on A means that, in general, the entanglement entropy in a gauge theory is inherently gauge dependent, even after the elimination of the gauge degrees of freedom in 2D QCD as we discussed earlier. We note that 't Hooft originally identified $A = \frac{1}{\epsilon^-}$ with an infrared cutoff [23], for which its removal from (47) will cause the contribution (46) to vanish. However, this is a particular gauge choice. In the $A = 0$ gauge (regular cutoff prescription) [29], the rainbow resummation in (47) is nonvanishing, with a renormalized squared mass $\tilde{m}^2 = m^2 - g^2N_c/\pi \geq 0$.

Since the gauge-dependent part of the self-energy does not change the short distance behavior, the small L behavior of the resummed entanglement entropy, in the planar approximation, is still dominated by the vacuum polarization diagram. It is gauge invariant (independent of A), and is equal to $\frac{N_c}{3}\ln\frac{L}{a}$. This result is reminiscent of the current-current two-point function which is given by the free fermion loop and of order N_c [31], an illustration of parton-hadron duality in 2D QCD. For $\tilde{m}^2 > 0$, the asymptotics of the central charge is seen to vanish as $N_c e^{-2\tilde{m}L}$, with the Renyi entropy dominated by the constant UV contribution (34) at large L, which is also gauge independent. These results are unaffected by the $\mathcal{O}(1)$ contributions as we discuss below.

Finally, we note that the case $m = 0$ is pathological with $\tilde{m}^2 < 0$ tachyonic. In this case, the left- and right-hand fermions decouple, with the fermionic propagator for the right-hand particle unchanged, while for the left particle it changes to

$$G^+(z) = e^{-ig^2N_cA|z|}\gamma^-\text{sign}(z)\int_0^\infty \frac{dk^+}{4\pi} e^{-ik^+|z| - i\frac{g^2N_c - i0}{\pi k^+}|z|}. \tag{48}$$

At long distance, (48) decays only polynomially as $1/z^{\frac{3}{2}}$, and the ensuing entanglement will decay also polynomially. On the other hand, since the right-hand fermion remains free, it will contribute only $\frac{N_c}{6}\ln\frac{L}{a}$ at long distances.

E. Order $\mathcal{O}(1)$ contribution

The $\mathcal{O}(1)$ contributions in the planar approximation resums the independent mesonic contributions to the entanglement entropy. The meson spectrum contains a would-be Goldstone mode that may shift the large distance part of the central charge from $\frac{N_c}{3}$ to $\frac{N_c}{3} + \frac{1}{3}$. We now show that this is not the case.

The $\mathcal{O}(1)$ contribution is illustrated in Fig. 6. In momentum space, it translates to

$$\ln Z_n|_{\text{double}} = 2 \times \frac{1}{2}\sum_k \left(\frac{2\pi k}{n}\right)^2 \int \frac{d^2k}{(2\pi)^2}\tilde{\Pi}^{00}(k) \times \frac{2 - 2\cos k^z L}{(k^z)^2}, \tag{49}$$

with $\tilde{\Pi}^{00}(k)$ given by

$$\tilde{\Pi}^{00}(k) = \int \frac{d^2p}{(2\pi)^2}\text{tr}S(p)\gamma^0 S(p+k)\gamma^0 S(p)\tilde{T}(p), \tag{50}$$

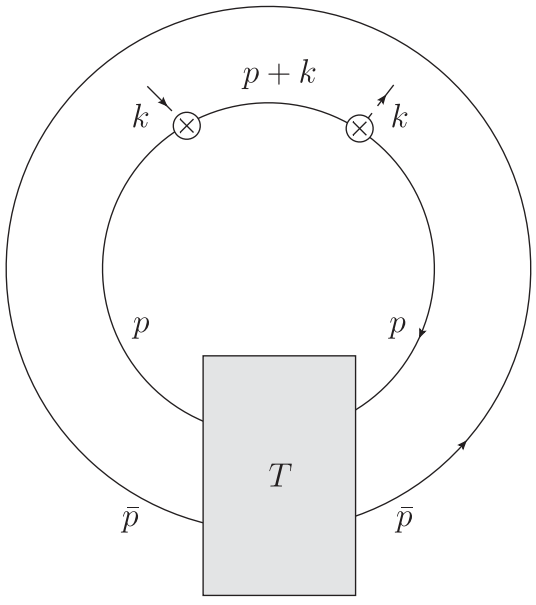

FIG. 6. The first nonvanishing double-loop contribution to Z_n. The shaded box is the amputated two-body planar amplitude. The crossed circles are the insertions of $\psi^\dagger\psi$.

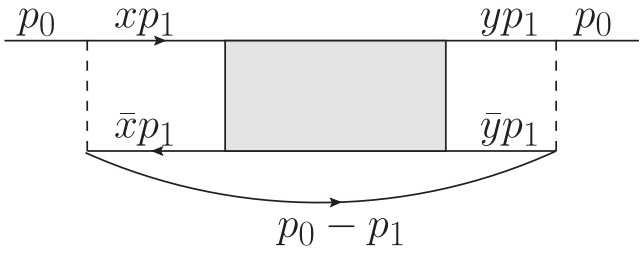

FIG. 7. The LF diagram for $\tilde{T}(p_0^+, p_0^-)$ where p_0^+ is positive (it is negative for the flipped antiquark line). The shaded box represents the equal incoming-outgoing LF time T matrix, and the dashed line represents the instantaneous gluon at equal LF time.

and

$$\tilde{T}^{aa'}_{\alpha\alpha'}(p) = \int \frac{d^2\bar{p}}{(2\pi)} T^{aa';bb}_{\alpha\alpha';\beta\beta'}(p,\bar{p}) S_{\beta'\beta}(\bar{p}). \tag{51}$$

Note that only the *forward but off-mass shell* part of the T matrix is needed. In light-cone gauge, $\tilde{T}$ follows from Fig. 7.

To evaluate this, one first notices that the equal incoming-outgoing time T matrix in LF gauge is simply given by

$$\begin{aligned} T(r^+, r^-, x, y) = {} & \frac{g^2}{(r^+)^2}\left(\frac{\pi r^2}{g^2 N_c} - \frac{\gamma-1}{x} - \frac{\gamma-1}{\bar{x}}\right)\delta(x-y) \\ & - \frac{g^2}{(r^+)^2}\left(\frac{\pi r^2}{g^2 N_c} - \frac{\gamma-1}{x} - \frac{\gamma-1}{\bar{x}}\right) \\ & \times \left(\frac{\pi r^2}{g^2 N_c} - \frac{\gamma-1}{y} - \frac{\gamma-1}{\bar{y}}\right) G(x,y,r^2), \end{aligned} \tag{52}$$

with $\gamma = \pi m^2/g^2 N_c$. The incoming + component momenta for the quark and the antiquark are xr^+ and $\bar{x}r^+$ and the total incoming LF energy is r^-. The mesonic Green's function $G(x,y,r^2)$ can be written in terms of the 't Hooft LF wave functions $\phi_n(x)$ for mesons with squared masses $m_n^2/g^2 N_c \sim n\pi$ (large n)

$$G(x,y,r^2) = \sum_n \frac{\varphi_n(x)\varphi_n(y)}{\frac{\pi r^2}{g^2 N_c} - \frac{\pi m_n^2}{g^2 N_c}}. \tag{53}$$

Thus, $\tilde{T}$ can be calculated as

$$\begin{aligned} \tilde{T}(p_0) = {} & \frac{(g^2 N_c)^2}{\pi N_c} \sum_n \int_0^1 dx \int_0^1 dy \int dp_1^- \\ & \times \int_0^{p_0^+} \frac{dp_1^+}{(2\pi)^2} \frac{\varphi_n(x)\varphi_n(y)}{(p_0^+ - xp_1^+)^2 (p_0^+ - yp_1^+)^2} \\ & \times \frac{(p_0 - p_1)^+}{(p_0 - p_1)^2 - m^2 + \frac{g^2 N_c}{\pi}} \frac{(p_1^+)^2}{(p_1)^2 - m_n^2} \end{aligned} \tag{54}$$

in the gauge with $A = 0$ (regular cutoff prescription). The above integral is convergent at $p_0^+ = p_1^+$ only if $\varphi_n(x) \sim x^\beta$ near the edges with $0 < \beta < 1$. The above can be calculated as

$$\begin{aligned} p_0^+ \tilde{T}(p_0) \equiv {} & \tilde{\Sigma}(p_0^2) \\ = {} & \frac{(g^2 N_c)^2}{\pi^2 N_c} \sum_n \int_0^1 dx dy dz \frac{\varphi_n(x)\varphi_n(y)}{(1-xz)^2(1-yz)^2} \\ & \times \frac{z}{p_0^2 - \frac{m_n^2}{z} - \frac{m^2 - \frac{g^2 N_c}{\pi}}{1-z} + i0}. \end{aligned} \tag{55}$$

This is actually the order $1/N_c$ correction to the quark-self energy. For an estimation, when $m^2 = 0$ there exists zero mass solution to the 't Hooft equation with $m_n = 0$; in this case the contribution reads

$$\begin{aligned} \Sigma(p_0^2) \sim {} & \frac{(g^2 N_c)^2}{\pi^2 N_c} \int_0^1 dx dy dz \frac{\varphi_0(x)\varphi_0(y)}{(1-xz)^2(1-yz)^2} \\ & \times \frac{z}{p_0^2 + \frac{\frac{g^2 N_c}{\pi}}{1-z} + i0}. \end{aligned} \tag{56}$$

If one uses $\phi_0 = 1$, the integral diverges logarithmically near $z = 1$. For small but finite m, the contribution is of order $\sqrt{g^2 N_c}/m$. When resummed into the fermion propagator, we have

$$S(p_0) = \frac{p_0^+}{p_0^2 - m^2 + \frac{g^2 N_c}{\pi} + \Sigma(p_0^2)} \tag{57}$$

in the $A = 0$ gauge (regular cutoff prescription). A rerun of the preceding arguments yields a central charge $\frac{N_c}{3}$, with no additional $\frac{1}{3}$ contribution from the would-be Golstone mode at long distances.

IV. SPATIAL ENTANGLEMENT IN EXCITED STATES

The present analysis can be generalized to any excited state $|N\rangle$. Using the pertinent interpolating fields to create the excited meson or baryon states, (24) readily generalizes to

$$Z_{N_n}(L) = \langle N_n | \mathcal{T} \exp\left[\sum_k i \frac{2\pi k}{n} \int_0^L ds n^\mu \epsilon_{\mu\nu} j_k^\nu(sn^\mu)\right] |N_n\rangle, \tag{58}$$

where $|N_n\rangle$ is a tensor product of $|N\rangle$, one for each replica copy,

$$|N_n\rangle = \bigotimes_{i=0}^{n-1} |N\rangle_i. \tag{59}$$

Moreover, if we choose n^μ to be along the LF$^-$ direction, then (58) is reminiscent of LF parton distribution functions.

A. Free parton on the light front

For a free fermion state of longitudinal momentum P^+ or $|N\rangle = b^\dagger_{P^+}|\Omega\rangle$, the contributions for different k factorize,

$$\ln Z_n = (1-n)S_n + \sum_{k=-\frac{n-1}{2}}^{\frac{n-1}{2}} \ln\left[\int_{-\Lambda^-/2}^{\Lambda^-/2} \frac{dxdy}{2\pi\Lambda^-}\frac{ie^{-i(x-y)}}{x-y+i0} \times \left(\frac{(x-\lambda+i0)(y-i0)}{(y-\lambda-i0)(x+i0)}\right)^{\frac{k}{n}}\right]. \tag{60}$$

Here R^- is the box size along LF$^-$, and $\Lambda^- = P^+R^-$ and $\lambda = P^+L^-$ the invariant lengths. In deriving (60), we used the bosonized representation for the fermion field $\psi_k \sim e^{i\phi_k}$ in (58). In the large LF box limit with $L^-/R^- \ll 1$, the kernel in (60) can be reduced,

$$\ln Z_n - (1-n)S_n = -\frac{4\lambda}{\Lambda^-}\sum_{k=-\frac{n-1}{2}}^{\frac{n-1}{2}} \sin^2\frac{k\pi}{n}\int_0^1 \frac{dxdy}{2\pi}\left[\frac{(1-x)y}{(1-y)x}\right]^{\frac{k}{n}} \times \frac{\sin\lambda(x-y)}{x-y}. \tag{61}$$

The details are in the Appendix. The entanglement entropy follows by performing the $n\to 1$ limit in (61), using the formula [5]

$$\lim_{n\to 1}\frac{1}{1-n}\sum_{k=-\frac{n-1}{2}}^{\frac{n-1}{2}} \sin^2\frac{k\pi}{n} z^{\frac{k}{n}} \sim -\lim_{n\to 1}\frac{2\pi^2(n-1)}{4\pi^2(n-1)^2+(z-1)^2} = -\pi^2\delta(z-1), \tag{62}$$

with the result

$$S = S(L^-) + \frac{4\pi^2\lambda}{\Lambda^-}\int_0^1 \frac{dxdy}{2\pi}\delta(x-y)y(1-y)\frac{\sin\lambda(x-y)}{x-y} = S(L^-) + \frac{\pi\lambda^2}{3\Lambda^-}. \tag{63}$$

$S(L^-)$ is the vacuum entanglement entropy discussed earlier. For large LF$^-$ intervals with invariant length $\lambda = P^+L^-$, the entanglement entropy of a free fermion on the LF is of order $\frac{\lambda^2}{\Lambda^-}$. For small intervals, it is dominated by the Logarithmic contribution from the vacuum in $S(L^-)$. In particular, for a free fermionic parton with the least longitudinal momentum $P^+ = \frac{2\pi}{R^-}$, (63) simplifies to

$$S = S(L^-) + \frac{2\pi^2}{3}\left(\frac{L^-}{R^-}\right)^2. \tag{64}$$

The additional contribution is the entanglement entropy for a primary state in a free conformal field theory [32] with $h=1$ and $\bar{h}=0$.

B. Free meson on the light front

Consider a bound meson state on the LF, with longitudinal momentum P^+,

$$|l\rangle = B^\dagger_{l,P^+}|\Omega\rangle \equiv \frac{1}{(\Lambda^-)^{\frac{1}{2}}}\int d\lambda_1 d\lambda_2 \varphi_l(\lambda_1,\lambda_2)\psi^\dagger(\lambda_1)\psi(\lambda_2)|\Omega\rangle, \tag{65}$$

with the coordinate space light-front wave function (LFWF)

$$\varphi_l(\lambda_1,\lambda_2) = \frac{1}{(2\pi)^2}\int_0^1 dx e^{-i\lambda_1 x - i\lambda_2(1-x)}\varphi_l(x) \tag{66}$$

and the normalization $\int dx|\varphi_l(x)|^2 = 1$. In the replica states constructed from (65), the replica partition function is

$$Z_n(l) = \langle\Omega|\prod_{j=0}^{n-1} B_{l,j}\exp\left[\sum_k i\frac{2\pi k}{n}\int_0^\lambda d\lambda'\psi_k^\dagger(\lambda')\psi_k(\lambda')\right] \times \prod_{j'=0}^{n-1} B^\dagger_{l,j'}|\Omega\rangle. \tag{67}$$

The corresponding entanglement entropy to leading order in $1/\Lambda^-$ is of the form (63). More specifically, it is proportional to λ^2, but dressed by the second moments of the quark/antiquark PDFs

$$S = S(L^-) + \frac{\pi\lambda^2}{3\Lambda^-}(\langle x_q^2\rangle_l + \langle x_{\bar{q}}^2\rangle_l) + \mathcal{O}\left(\frac{1}{\Lambda^{-2}}\right), \tag{68}$$

where

$$\langle x_q^2\rangle_l = \int_0^1 dx x^2|\varphi_l(x)|^2, \qquad \langle x_{\bar{q}}^2\rangle_l = \int_0^1 dx\bar{x}^2|\varphi_l(x)|^2, \tag{69}$$

are the second moments of the quark and antiquark PDFs. The higher and even moments of the PDFs are suppressed by further powers of $1/\Lambda^-$ in the entanglement entropy (68). For the meson state in the Schwinger model, each of the second moments is $\frac{1}{3}$.

To derive (68), it is best to use a diagrammatic analysis of (67) as illustrated in Fig. 8. The disconnected bubbles where the meson operators contract among themselves exponentiate and contribute to the vacuum state entanglement. So we need to consider only the connected diagrams where the combination $\psi_i^\dagger\psi_i$ from the external state contracts with $\psi_k^\dagger\psi_k$ from the vector operator in the exponent. We now note

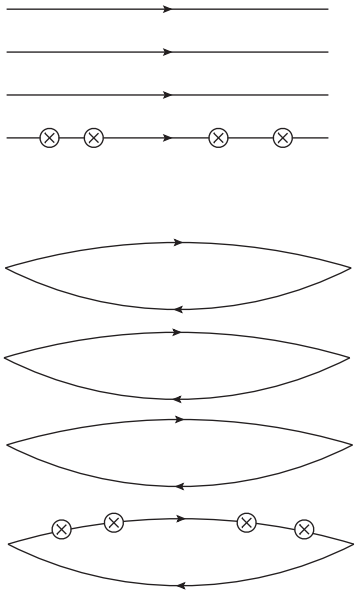

FIG. 8. The leading $1/\Lambda^-$ contribution to the spatial entanglement for n-replicated fermion (upper) and n-replicated meson states (lower). The crossed circles denote the vector current operator insertions. To leading order in $1/\Lambda^-$, $n-1$ pairs of the replicated external states contract with themselves, leaving only one pair for the vector current insertion. To leading order in $n-1$, no additional insertion is needed.

that each time a $\psi_i^\dagger\psi_i$ from the external state contracts with $\psi_k^\dagger\psi_k$ from the operator insertion, a suppression factor $1/\Lambda^-$ arises. Hence, the leading $1/\Lambda^-$ contribution consists of $n-1$ pairs of external states contracted among themselves, with the remaining pair contracted with $\psi_k^\dagger\psi_k$ from the vector operator insertion.

For a replicated fermion in Fig. 8 (top), this contribution is the trace over the i fields, which readily converts to the sum over the k fields. This reproduces the second term in (A2). The extra -1 corresponds to the subtraction of the term with no insertions.

This observation extends to the replicated meson state as well. The leading contribution is shown in Fig. 8 (bottom). For a generic n, the operators can be inserted simultaneously on the fermion/antifermion lines. To obtain the linear contribution in $n-1$, one needs the insertions exclusively on either the fermion or the antifermion legs, but not both. In this case one reproduces the above free fermion contributions, but weighted over the LFWF of the meson,

$$S - S(L^-) = \frac{1}{\Lambda^-}\int_0^1 dx|\varphi_n(x)|^2(F_{\rm single}(x\lambda) + F_{\rm single}(\bar{x}\lambda)), \tag{70}$$

where $F_{\rm single}(\lambda) = \frac{\lambda^2\pi}{3}$ is the fermion contribution. This is (68) and concludes our derivation. One should mention that although the above derivation is for a free replicated meson state, it can be extended to 2D QCD, using the large N_c power-counting methods detailed above.

We note that for spacelike cuts, the replica partition function (67) can be regarded as a meson-meson correlation function, with replicated fermionic vector charge insertions. In the limit where the meson sources are asymptotically separated, it is in general a function of the form $Z_n(P\cdot L, P\cdot R, L^2, R^2)$ and can be probed on an Euclidean lattice in the same spirit as the quasi-PDF approach in [33,34] for parton densities. For say large P^z and fixed spatial cut $L^z < R^z =^4 \sqrt{V_4}$, the second moment of the quark PDF in a meson state can be read from the coefficient of the Renyi entropy that scales like $1/P^zR^z$.

C. Coherent meson state on the light front

In a general bosonic coherent state

$$|\xi\rangle = e^{-\frac{|\xi^2|}{2}-\xi B_l^\dagger}|\Omega\rangle$$

constructed using (65) with ξ complex valued, the replica partition function is

$$Z_n(\xi) = \prod_k Z_k(\xi) = \prod_k e^{-|\xi^2|}\langle\Omega|\exp[-\xi^* B_l] \times \exp\left[i\frac{2\pi k}{n}\int_0^\lambda d\lambda'\psi^\dagger(\lambda')\psi(\lambda')\right]\exp[-\xi B_l^\dagger]|\Omega\rangle. \tag{71}$$

For 2D QCD the reduction of (71) in terms of the LFWF $\varphi_l(x)$ is straightforward but tedious. This construction maybe used to probe for many-body correlations. Equation (71) simplifies considerably for 2D QED or the Schwinger model. Indeed, for the latter B_l is nothing but the bosonized field, and (71) can be reduced by bosonization to

$$\ln Z_k(\xi) = \ln Z_k - \frac{2\xi k}{n}\frac{\sqrt{2\pi}}{\sqrt{P^+L^-}}\sin\lambda, \tag{72}$$

where Z_k is the vacuum contribution. After summing over k, all the k-dependent terms cancel out, with only the vacuum contribution remaining. For the Schwinger model, the bosonic coherent state has the same LF-spatial entanglement as that of the vacuum.

V. HOLOGRAPHIC DUAL CONSTRUCTION

In this section, we will construct a soft wall holographic dual to two-dimensional QCD, using the bottom-up approach. Using the Ryu-Takayanagi proposal [25], we will derive the entanglement entropy geometrically. We will illustrate the derivation by recalling the construction for two-dimensional CFT with an AdS_3 gravity dual, and then extend it to the nonconformal case of two-dimensional QCD using soft-wall AdS_3.

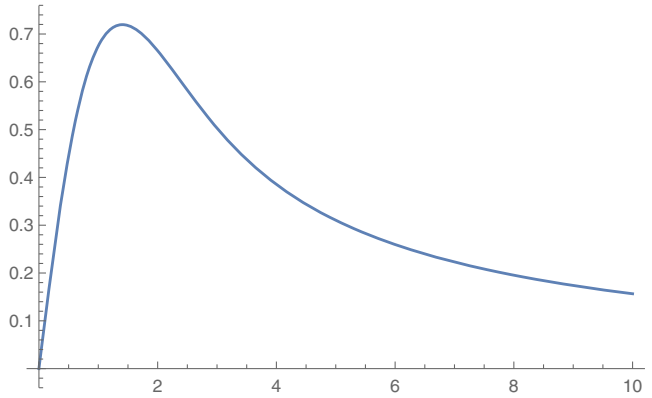

FIG. 9. $F(\tilde{z}_m)$ in (85) as a function of $\tilde{z}_m$, with a maximum at $\tilde{z}_m \sim 1.4$.

A. AdS_3

Two-dimensional conformal theories map onto AdS_3, with a central charge $c = 3R/2G_3$, with R the radius of AdS_3, and G_3 the bulk Newton gravitational constant. In this regime, the entanglement entropy for the single spatial cut $L = |a_1 - a_2|$ can be read in bulk using the Ryu-Takayanagi proposal [25]

$$S = \frac{\gamma_L}{4G_3} \to \frac{c}{3}\log\left(\frac{R}{a}\sin\left(\frac{\pi L}{R}\right)\right) \tag{73}$$

with γ_L the length of the bulk AdS_3 geodesic. In two dimensions $G_3 = g_s l_s$ and $R/G_3 = (R/l_s)/g_s$, with the string length l_s. The string coupling is $g_s \sim 1/N_c$, with the $1/N_c$ universal from the genus expansion. For conformal fermions in the fundamental representation, we expect $R/l_s = \# > 1$ (below # is of order 1), with $c = N_c$.

In Poincare coordinates with line element

$$ds^2 = \frac{R^2}{z^2}(-dt^2 + dx^2 + dz^2) \tag{74}$$

the geodesic is a semicircle $\dot{x}^2 + \dot{z}^2 = (L/2)^2$,

$$(x(s), z(s)) = \frac{L}{2}(\cos s, \sin s) \tag{75}$$

sustained by the single-cut end-points $\pm L/2$ on the Minkowski boundary at $z = a \ll L$ (range $2a/L \le s \le \pi - 2a/L$). The geometric entanglement entropy is the length of the geodesic in Planck units

$$S = \frac{1}{4G_3}\int_{2a/L}^{\pi/2} ds\sqrt{g_{MN}\dot{x}^M\dot{x}^N} = \frac{R}{2G_3}\int_{2a/L}^{\pi/2}\frac{ds}{\sin s} = \frac{R}{2G_3}\log\left(\frac{\pi L}{a}\right). \tag{76}$$

B. Soft-wall AdS_3

Assume now the geometry is controlled by a soft-wall AdS_3

$$ds^2 = \frac{e^{-\kappa^2 z^2}}{z^2}(dz^2 + dx^2 - dt^2), \tag{77}$$

where $\kappa^2 \propto g^2 N_c$ plays the role of the "string tension." The minimal surface is parametrized by

$$(x, z, t) = (x(s), z(s), 0), \tag{78}$$

where $0 \le s \le 1$. The two-dimensional bulk action is

$$S = \int ds \frac{e^{\frac{-\kappa^2 z^2}{2}}}{z}\sqrt{\dot{x}^2 + \dot{z}^2}, \tag{79}$$

for which the minimal surface can be chosen to satisfy

$$\frac{\dot{x}}{\sqrt{\dot{x}^2 + \dot{z}^2}}\frac{e^{-\frac{\kappa^2 z^2}{2}}}{z} = \alpha, \tag{80}$$

$$\dot{x}^2 + \dot{z}^2 = \beta^2, \tag{81}$$

which leads to

$$\dot{z}^2 = \alpha^2\beta^2(z_m^2 e^{\kappa^2 z_m^2} - z^2 e^{\kappa^2 z^2}), \tag{82}$$

$$\dot{x} = \alpha\beta z e^{\frac{\kappa^2}{2}}. \tag{83}$$

Here z_m is the maximal value of z attained at $s = \frac{1}{2}$, which satisfies

$$\frac{L}{2} = \int_0^1 ds\dot{x} = \int_0^{z_m} dz \frac{z e^{\frac{\kappa^2 z^2}{2}}}{\sqrt{z_m^2 e^{\kappa^2 z_m^2} - z^2 e^{\kappa^2 z^2}}}. \tag{84}$$

For small L (84) reproduces the circular solution in AdS_3 discussed above. For large L, we define $\tilde{z}_m = z_m\kappa$ and $\tilde{L} = L\kappa$, so that

$$\frac{\tilde{L}}{2} = \tilde{z}_m\int_0^1 dt \frac{t}{\sqrt{e^{\tilde{z}_m^2(1-t^2)} - t^2}} \equiv F(\tilde{z}_m). \tag{85}$$

See Fig. 9 for a depiction of the function $F(z)$. For small $\tilde{z}_m \ll 1$, $F(\tilde{z}_m) = \tilde{z}_m$ and the circular solution follows. However, a maximum develops for $\tilde{z}_m \sim 1.4$, so that $F(\tilde{z}_m) \le 0.72$. The connected solutions only exist for small L, at strong 't Hooft coupling

$$L \le \frac{1.44}{\kappa} \sim \frac{1.44}{\sqrt{g^2 N_c}}. \tag{86}$$

For large L the minimal surface cannot be smoothly connected to the small L solution. A similar observation

was also made for D-branes in higher dimensions, where at large L the solution was argued to be made of two disjoint in-falling geodesics [35]. For the soft-wall model, this disconnected geometry can be approximated by

$$S \approx 2 \times \frac{R}{4G_3}\int_a^{z_m}\frac{dz}{z} = \frac{R}{2G_3}\log\left(\frac{z_m}{a}\right). \tag{87}$$

The net entanglement entropy is a competition between the circular (76) and disjoint (87) geometries,

$$\Delta S = S(\kappa L \ll 1) - S(\kappa L \gg 1) = \frac{R}{2G_3}\log\left(\frac{\pi L}{z_m}\right) \to \frac{N_c}{3}\log\left(\frac{\pi L}{z_m}\right). \tag{88}$$

The Ryu-Takayanagi entropies for small (76) and large (87) spatial cuts are in agreement with the perturbative Renyi entropy (34), and its nonperturbative analog $m \to \tilde{m}$ at large N_c, respectively.

This interpolation between a connected surface for small cuts and a disconnected surface for large cuts is similar to the observation put forth in [35], for several holographic constructions dual to 4D conformal and confining gauge theories. However, the chief difference in our case stems from the fact that 2D QCD at large N_c, confines at all distance scales. The geometrical change we observed is not related to a Hagedorn-like growth in the confined meson spectrum as argued in 4D QCD in [35], as there is none in 2D, but is rather a reflection of parton-hadron duality for small intervals in 2D QCD.

VI. CONCLUSIONS

We have shown how to extend the replica construction to Minkowski space-time signature and use it to derive a general formula for the replica partition function in the vacuum state. Our result applies to a large class of interacting theories with fermions with or without gauge fields for any space-time cut and in arbitrary dimensions. When analytically continued to Euclidean signature, our result can be explicitly reduced to the standard result, using bosonization.

In the presence of gauge interactions, spatial entanglement as described by our replica partition function is in general gauge dependent, a result of gluing fermionic fields valued in different replica strips along the spatial cut. However, the ensuing Renyi entropy for small or large cuts can still exhibit gauge-independent contributions. We have shown that this is the case in two-dimensional QCD.

For small spacelike cuts, the Renyi entropy was shown to follow from the charge density correlation function, which is fixed at a short distance by the 2D axial anomaly. The central charge is $\frac{N_c}{3}$ and gauge independent. At large distances, the perturbative arguments break down. Using the planar expansion, we showed that the leading $\mathcal{O}(N_c)$ contribution is tied to the rainbow dressed quark propagator, which is explicitly gauge fixing dependent. However, for large cuts, this contribution vanishes exponentially with the distance L, leaving behind only the gauge-independent UV constant contribution. The mesonic $\mathcal{O}(1)$ contributions do not change this result.

Our results are not limited to the vacuum state. We have shown that spatial entanglement on the light front can be extended to any hadron state, with minimal changes to our central result for the replica partition function. The result is reminiscent of LF wave functions, which shows a direct relationship between the Renyi entropy of an excited hadron and its parton distribution on the light front. Conversely and for spacelike intervals, the even moments of the quark PDFs in a hadron state in 2D QCD can be extracted from the Renyi entropy at large momentum. This observation extends to 4D QCD both in the continuum and on an Euclidean lattice.

Using a bottom-up soft-wall model for 2D QCD in AdS_3, we have shown that the Ryu-Takayanagi geometrical entropy interpolates between the known conformal AdS_3 result for a small spatial cut and a constant but UV sensitive result for a large spatial cut. This result is in total agreement with the Renyi entropy, following from our new replica construction. Although 2D QCD at large N_c is not conformal at all distance scales, the agreement with the conformal AdS_3 result for small intervals illustrates the parton-hadron duality at work in theories with confinement.

ACKNOWLEDGMENTS

This work is supported by the Office of Science, U.S. Department of Energy, under Contract No. DE-FG-88ER40388, and by the Priority Research Area SciMat and DigiWorlds under the program Excellence Initiative—Research University at the Jagiellonian University in Kraków.

APPENDIX: DETAILS IN THE KERNEL REDUCTION

In the large Λ^- limit one can split the kernel (60) into

$$\int_{-\Lambda^-/2}^{\Lambda^-/2}\frac{dxdy}{2\pi\Lambda^-}\frac{ie^{-i(x-y)}}{x-y+i0}\frac{(x-\lambda+i0)(y-i0)}{(y-\lambda-i0)(x+i0)}\Big)^{\frac{k}{n}} = 1 + \frac{1}{\Lambda^-}\int_{-\Lambda^-/2}^{\Lambda^-/2}\frac{dxdy}{2\pi}\frac{ie^{-i(x-y)}}{x-y+i0} \times \left[\left(\frac{(x-\lambda+i0)(y-i0)}{(y-\lambda-i0)(x+i0)}\right)^{\frac{k}{n}} - 1\right] \tag{A1}$$

and

$$\ln Z_n = (1-n)S_n + \frac{1}{\Lambda^-}\sum_{k=-\frac{n-1}{2}}^{\frac{n-1}{2}} \int_{-\Lambda^-/2}^{\Lambda^-/2} \frac{dxdy}{2\pi} \frac{ie^{-i(x-y)}}{x-y+i0}\left[\left(\frac{(x-\lambda+i0)(y-i0)}{(y-\lambda-i0)(x+i0)}\right)^{\frac{k}{n}} - 1\right]. \tag{A2}$$

The reduction of (A2) follows by noting that the bracket is of the form

$$F(z) = \ln(z-\lambda) - \ln z, \tag{A3}$$

with a branch cut along $[0,\lambda]$ with discontinuity $2\pi i$. The ensuing integral follows by contour

$$\begin{aligned}
&\int_{-\Lambda^-/2}^{\Lambda^-/2} \frac{dxdy}{2\pi} \frac{ie^{-i(x-y)}}{x-y+i0}\left[\left(\frac{(x-\lambda+i0)(y-i0)}{(y-\lambda-i0)(x+i0)}\right)^{\frac{k}{n}} - 1\right] \\
&= \int_{-\Lambda^-/2}^{\Lambda^-/2} \frac{dxdy}{2\pi} \frac{ie^{-i(x-y)}}{x-y+i0} e^{\frac{k}{n}F(x+i0)-\frac{k}{n}F(y-i0)} \\
&= \int_{-\Lambda^-/2}^{\Lambda^-/2} \frac{dxdy}{2\pi} \frac{ie^{-i(x-y)}}{x-y+i0}\left[e^{\frac{k}{n}F(x-i0)-\frac{k}{n}F(y-i0)} + \delta A(x) e^{-\frac{k}{n}F(y-i0)}\right] \\
&= \Lambda^- + \int_{-\Lambda^-/2}^{\Lambda^-/2} \frac{dxdy}{2\pi} \frac{ie^{-i(x-y)}}{x-y+i0} \delta A(x) e^{-\frac{k}{n}F(y-i0)} \\
&= \Lambda^- + \int_{-\Lambda^-/2}^{\Lambda^-/2} \frac{dxdy}{2\pi} \frac{ie^{-i(x-y)}}{x-y+i0} \delta A(x)\delta B(y) + \int_{-\Lambda^-/2}^{\Lambda^-/2} dx \delta A(x) e^{-\frac{k}{n}F(x+i0)},
\end{aligned} \tag{A4}$$

with

$$\delta A(x) = e^{\frac{k}{n}F(x-i0)} - e^{\frac{k}{n}F(x+i0)} = (e^{-\frac{2\pi k}{n}i} - 1) e^{\frac{k}{n}F(x+i0)} \theta(x)\theta(\lambda - x), \tag{A5}$$

$$\delta B(y) = e^{-\frac{k}{n}F(y+i0)} - e^{-\frac{k}{n}F(y-i0)} = (1 - e^{\frac{2\pi k}{n}i}) e^{-\frac{k}{n}F(y+i0)} \theta(y)\theta(\lambda - y). \tag{A6}$$

Using the relation assignment $\frac{1}{x-y+i0} = \mathrm{PV}.\frac{1}{x-y} - i\pi\delta(x-y)$, we obtain (61).

[1] Mark Srednicki, Entropy and Area, Phys. Rev. Lett. **71**, 666 (1993).
[2] Christoph Holzhey, Finn Larsen, and Frank Wilczek, Geometric and renormalized entropy in conformal field theory, Nucl. Phys. **B424**, 443 (1994).
[3] Curtis G. Callan, Jr. and Frank Wilczek, On geometric entropy, Phys. Lett. B **333**, 55 (1994).
[4] Pasquale Calabrese and John L. Cardy, Entanglement entropy and quantum field theory, J. Stat. Mech. (2004) P06002.
[5] H. Casini, C. D. Fosco, and M. Huerta, Entanglement and alpha entropies for a massive Dirac field in two dimensions, J. Stat. Mech. (2005) P07007.
[6] M. B. Hastings, An area law for one-dimensional quantum systems, J. Stat. Mech. (2007) P08024.
[7] Pasquale Calabrese and John Cardy, Entanglement entropy and conformal field theory, J. Phys. A **42**, 504005 (2009).
[8] H. J. Bremermann, in *Proceedings of the Fifth Berkeley Symposium on Mathematical Statistics and Probability*, edited by Lucien M. Le Cam and Neyman Jerzy (University of California Press, Berkeley, 1967), Vol. 3.
[9] Jacob D. Bekenstein, Energy Cost of Information Transfer, Phys. Rev. Lett. **46**, 623 (1981).
[10] Adam M. Kaufman, M. Eric Tai, Alexander Lukin, Matthew Rispoli, Robert Schittko, Philipp M. Preiss, and Markus Greiner, Quantum thermalization through entanglement in an isolated many-body system, Science **353**, 794 (2016).
[11] Alexander Stoffers and Ismail Zahed, Holographic pomeron and entropy, Phys. Rev. D **88**, 025038 (2013).
[12] Yachao Qian and Ismail Zahed, Stretched string with self-interaction at the Hagedorn point: Spatial sizes and black holes, Phys. Rev. D **92**, 105001 (2015).
[13] Jürgen Berges, Stefan Floerchinger, and Raju Venugopalan, Entanglement and thermalization, Nucl. Phys. **A982**, 819 (2019).
[14] Adrien Florio and Dmitri E. Kharzeev, Gibbs entropy from entanglement in electric quenches, Phys. Rev. D **104**, 056021 (2021).
[15] Yizhuang Liu, Maciej A. Nowak, and Ismail Zahed, Entanglement entropy and flow in two-dimensional QCD: Parton and string duality, Phys. Rev. D **105**, 114027 (2022).

[16] Dmitri E. Kharzeev and Eugene M. Levin, Deep inelastic scattering as a probe of entanglement, Phys. Rev. D **95**, 114008 (2017).
[17] Yizhuang Liu, Maciej A. Nowak, and Ismail Zahed, Rapidity evolution of the entanglement entropy in quarkonium: Parton and string duality, Phys. Rev. D **105**, 114028 (2022).
[18] Yachao Qian and Ismail Zahed, Stretched string with self-interaction at high resolution: Spatial sizes and saturation, Phys. Rev. D **91**, 125032 (2015).
[19] Edward Shuryak and Ismail Zahed, Regimes of the pomeron and its intrinsic entropy, Ann. Phys. (Amsterdam) **396**, 1 (2018).
[20] Yizhuang Liu and Ismail Zahed, Entanglement in Regge scattering using the AdS/CFT correspondence, Phys. Rev. D **100**, 046005 (2019).
[21] Nestor Armesto, Fabio Dominguez, Alex Kovner, Michael Lublinsky, and Vladimir Skokov, The color glass condensate density matrix: Lindblad evolution, entanglement entropy, and Wigner functional, J. High Energy Phys. 05 (2019) 025.
[22] Gia Dvali and Raju Venugopalan, Classicalization and unitarization of wee partons in QCD and gravity: The CGC-black hole correspondence, Phys. Rev. D **105**, 056026 (2022).
[23] Gerard 't Hooft, A two-dmensional model for mesons, Nucl. Phys. **B75**, 461 (1974).
[24] I. Bars, A quantum string theory of hadrons and its relation to quantum chromodynamics in two dimensions, Nucl. Phys. **B111**, 413 (1976).
[25] Shinsei Ryu and Tadashi Takayanagi, Holographic Derivation of Entanglement Entropy from AdS/CFT, Phys. Rev. Lett. **96**, 181602 (2006).
[26] Mikhail Goykhman, Entanglement entropy in 't Hooft model, Phys. Rev. D **92**, 025048 (2015).
[27] A. Armoni, Y. Frishman, and J. Sonnenschein, Massless QCD_2 from current constituents, Nucl. Phys. **B596**, 459 (2001).
[28] Vincenzo Alba, Maurizio Fagotti, and Pasquale Calabrese, Entanglement entropy of excited states, J. Stat. Mech. (2009) P10020.
[29] Martin B. Einhorn, Form factors and deep inelastic scattering in two-dimensional quantum chromodynamics, Phys. Rev. D **14**, 3451 (1976).
[30] Y. Frishman, Non-Abelian gauge theory in two-dimensions, Nucl. Phys. **B148**, 74 (1979).
[31] Curtis G. Callan, Jr., Nigel Coote, and David J. Gross, Two-dimensional Yang-Mills theory: A model of quark confinement, Phys. Rev. D **13**, 1649 (1976).
[32] Miguel Ibanez Berganza, Francisco Castilho Alcaraz, and German Sierra, Entanglement of excited states in critical spin chains, J. Stat. Mech. (2012) P01016.
[33] Xiangdong Ji, Parton Physics on a Euclidean Lattice, Phys. Rev. Lett. **110**, 262002 (2013).
[34] Xiangdong Ji, Parton physics from large-momentum effective field theory, Sci. China Phys. Mech. Astron. **57**, 1407 (2014).
[35] Igor R. Klebanov, David Kutasov, and Arvind Murugan, Entanglement as a probe of confinement, Nucl. Phys. **B796**, 274 (2008).